

## EDDY CURRENT SCANNING AT FERMILAB\*

C. Boffo<sup>#</sup>, P. Bauer, M. Foley, FNAL, Batavia, IL 60510, U.S.A.  
 A. Brinkmann, DESY, Hamburg, Germany  
 J. Ozelis, TJNAF, Newport News, VA 23606, U.S.A.

### Abstract

In the framework of SRF cavity development, Fermilab is creating the infrastructure needed for the characterization of the material used in the cavity fabrication. An important step in the characterization of “as received” niobium sheets is the eddy current scanning. Eddy current scanning is a non-destructive technique first adopted and further developed by DESY with the purpose of checking the cavity material for sub-surface defects and inclusions.

Fermilab has received and further upgraded a commercial eddy current scanner previously used for the SNS project. The upgrading process included developing new filtering software. This scanner is now used daily to scan the niobium sheets for the Fermilab third harmonic and transverse deflecting cavities.

This paper gives a status report on the scanning results obtained so far, including a discussion of the typology of signals being detected. We also report on the efforts to calibrate this scanner, a work conducted in collaboration with DESY.

### THE EDDY CURRENT SCANNER

The use of Eddy Current Scanners (ECS) in SRF was introduced by DESY, [1], as a systematic approach for the quality control of the Niobium used for cavity fabrication.

The basic principle behind this device is to utilize the alteration of the eddy current field in a double coil sensing probe to detect inclusions and defects embedded under the surface of the material.

The device now operating at Fermilab [2], shown in Fig. 1, was developed by BAM and built under BAM license by FER-PA (Germany), used during the SNS



Fig. 1 SNS Eddy current scanner setup

cavity fabrication program, and loaned to Fermilab in 2004. In this particular machine, the sample is fixed to a rotating table, which is attached to a linear slider, while the sensing head is kept fixed. This setup is specifically designed to scan disks: at a given relative radial position of the head, the sample rotates several times allowing for data acquisition, then the relative position of the head is changed by sliding the table and the data acquisition is repeated over a different circumference. The head generates two signals at different frequencies for simultaneous investigation over two depths. The signals are then digitalized and transferred to a PC where the data are stored and represented in form of pictures as shown in Fig. 2.

A particular feature of the BAM scanner design is the pneumatic probe levitation. Compressed air is blown through the probe onto the sample, which allows the spring mounted probe to float over the sample. This feature stabilizes the probe to sample distance allowing the probe to instantaneously adapt to irregularities of the sample surface. Since the rotating table uses a vacuum clamping system intended for the SNS blanks, a fixture, visible in Fig. 1 was designed to adapt the machine to the small Niobium disks for the 3.9 GHz cavities developed at Fermilab.

Initial tests showed that this machine was not reaching the sensitivity of the one at DESY, limiting the overall detection capabilities. For this reason the device underwent a number of hardware and software upgrades.

### UPGRADES

The key elements for the ECS performances are the distance between sensing head and sample, and its stability. In general the nearer the head to the sample, the stronger and sharper is the signal generated by a defect. To increase the overall positional control, the alignment capabilities of the device have been improved.

Furthermore the output of the data analysis software is a picture, limiting the post processing to image handling algorithms. A separate filter application, based directly on the acquired data was therefore developed to improve the scanning resolution.

### Hardware

The distance of the sensing head with respect to the sample is kept stable by the pneumatic probe levitation system. In order to minimize the distance one must be capable of precisely adjusting the head height and pitch with respect to the sample. For this purpose the head was attached to a micrometric adjusting stage allowing reducing the gap to few  $\mu\text{m}$ . At this distance the flatness

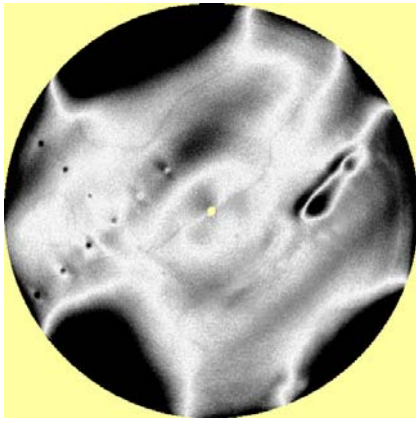


Fig. 2 FNAL scan of the DESY calibration disk

and the thickness variation of the sample become the limiting factor and cannot be easily overcome.

Additional improvements were obtained using a centering fixture to precisely align the sample holder to the rotating table. This feature allows minimizing the distortion in the results related to the sample edge effect. When the probe is not completely above the sample, strong signals are generated, which reduce the scanning resolution.

### Software

If the system is properly calibrated the sample-head distance variations and the inclusions or defects should be separated into the real and in the imaginary portions of the complex number obtained in each scanned point [3]. Often, however, this is not the case. Moreover the distance variations limit the capability of effectively detecting the defects. This problem is related to the way the scanning results are visualized, namely in a picture of the scanned area where the color of each point (usually in gray scale) is proportional to the signal detected. The color range is adjusted to the maximum and minimum values detected. If for example the signal related to a probe-sample distance variation is very strong, the signals related to defects are drowned in the noise and not visible. In order to minimize this effect a new filtering application was developed [4].

Fig. 3 shows the scanned data along a radius with a typical defect (red oval) sitting on top of the distance variation effect (green line). The new application applies a band-pass FIR filter to eliminate the long-range distance variation effect and therefore resolve more clearly the defect as shown in Fig. 4. An additional improvement is obtained by squaring all the signals and attenuating by a factor of 100 the values below one standard deviation from the mean. In order to normalize the color-range in the image of the filtered results, a row with a standard defect is added to the bottom of the data matrix. This position in the data matrix corresponds to the innermost circumference of the sample and is practically invisible in the final result.

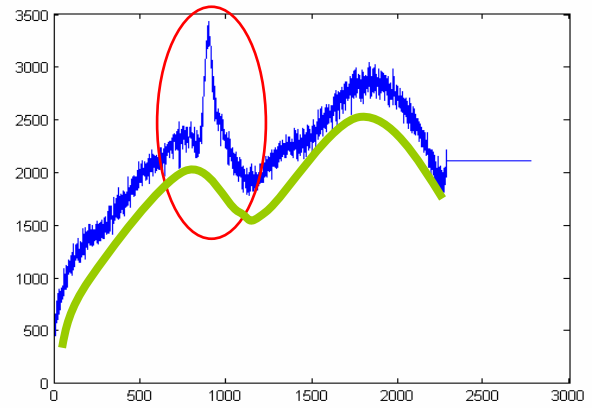


Fig. 3 Data along a radius of a sample with typical defect (red) on top of the distance variation effect (green).

## CALIBRATION

A calibration sample from DESY was used to compare the sensitivity of the ECS of both laboratories [5]. This calibration sample is a ~2.5 mm thick ~25 cm square niobium sheet supplied by Wah-Chang. It contains eleven sub-surface defects. Out of the eleven, two are just holes and nine are holes of different diameter (120  $\mu\text{m}$  – 230  $\mu\text{m}$ ) filled with tantalum powder, subsequently melted and covered using e-beam welding. The FNAL and the DESY scans of the calibration disc after filtering are shown in Fig. 5. In order to further improve the FNAL results several parameters have been optimized as described in the following paragraphs.

### Turntable velocity

In order to reduce mechanical vibration, the turntable speed was reduced from 170 rpm to 105 rpm by replacing the pulley on the motor side of the drive mechanism. Comparative measurements did not reveal any significant improvement.

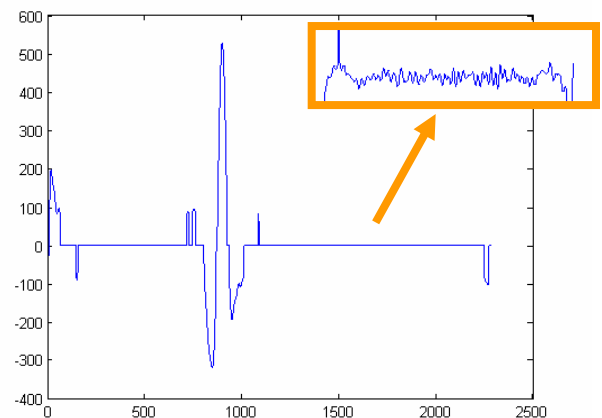


Fig. 4 Defect shown in Fig. 3 as it appears after the filter application.

## Probe Air Pressure

The nominal setting of the probe air pressure is  $\sim 2.0$  bar. The air pressure affects the pneumatic probe levitation, thus modifying distance between sample and probe and the capability of the probe to react to sample irregularities (thickness variations, bumps...etc). This issue makes the tests at different probe air pressure difficult since the probe height must be readjusted each time adding uncertainty to the comparison. The goal of the test was to check if the head, working at lower pressure, was able to better follow the sample topology. Tests were performed at pressures between 1.6 bar and 2.0 bar, giving similar results with the exception of the 1.6 bar case which showed lower sensitivity.

## Number of Measurement Points

The number of points acquired during the scan is a very important parameter in terms of device sensitivity. Due to the distance of the probe from the surface and the shape of the eddy current fields generated, the size of the signal for a  $100\ \mu\text{m}$  defect is of the order of 1 mm. The number of points acquired per turn of the table does not affect the scanning time since the rotation speed is fixed, but the track-to-track scanning distance does have a linear effect on the scanning time. Furthermore the more the number of points the bigger are the files generated and the longer are the filtering times. Beyond a minimum number of points threshold, however, the major limiting element is the data representation technology. Printers and monitors may not be able to resolve the smallest defects that the scanner can detect.

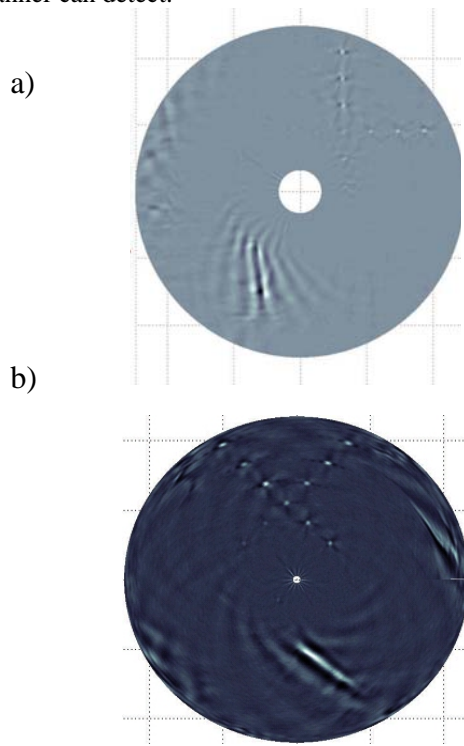


Fig. 5 DESY calibration disk after filter application  
a) DESY and b) FNAL

Our experiments showed that the combination of 1600 points per track and  $100\ \mu\text{m}$  track spacing is optimal, producing a reasonable file dimension of  $\sim 14$  Mb which needs a filtering time similar to the scanning one. In the case of a 25 cm diameter disc these settings lead to an azimuthal spacing of  $\sim 0.5\text{--}0.05$  mm from the outer to the inner edges of the scanning area.

## Filtering

The filter application described above was of course a major element in the improvement of the SNS scanner resolution. Shown in Fig. 5 is a demonstration of its power applied to the calibration disc measurement obtained with the DESY scanner.

## SCAN RESULTS

The ECS, after optimization, was employed to scan up to 90 disks to be used for the production of 6 FNAL 3<sup>rd</sup> harmonic cavities [6,7]. Each disk was visually inspected on both sides using a magnifying glass, afterwards it was scanned and the results filtered. The results can be summarized as follows: out of the last 90 discs scanned, 21 (23%) give no defect related signal and 22 discs (25%) give signals on both sides; 69 discs (76%) have at least one side giving a signal. 74 sides (41%) have visible pits (of which only 25% appear in the eddy current scans), 112 sides (62%) have scratches, and 27 sides (15%) have roller marks (which only appear in the eddy current scans). Results are also shown in Fig. 6a and 6b.

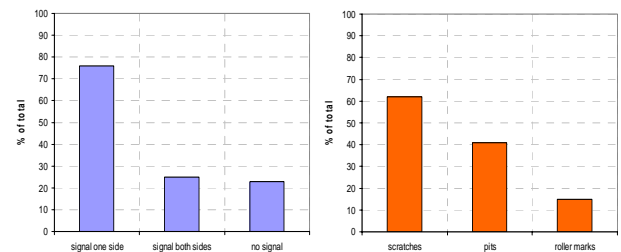


Fig. 6 Results of ECS on  $\sim 90$  disks to be used in 6 FNAL 3<sup>rd</sup> Harmonic cavities.

## SURFACE DEFECTS INVESTIGATION

Scratches and pits, which are mostly visible with the naked eye, are the dominant defects detected both by the scanner and by the visual inspection. Profilometric measurements [7] were introduced to characterize the pits present on the surface of the disks. Measurements were performed on six disks presenting several pits each, using a Taylor Hobson Talysurf Intra device equipped with a  $2\ \mu\text{m}$  radius diamond chisel. The measured pits dimensions varied between 0.2 and 0.5 mm in diameter and between 10 and  $90\ \mu\text{m}$  in depth. Fig. 7 shows a typical result: the rich topology of the profile suggests that these pits could be the result of imprinting of grains, previously detached from the Niobium, sticking to the cylinders during the

rolling process. Additional chemical analysis of the first micron on the surface of the pits using EDX confirmed that the chemical composition of these craters is the same as the rest of the disk. A number of disks have been BCP etched to check if the defects would be eliminated during the cavity production process (which includes a minimum of 120  $\mu\text{m}$  surface removal by chemistry). The results showed that not all defects are eliminated. We therefore recommend that the sides of the disks, which show a signal in the ECS (usually the case for the deepest pits and “roller marks”), should not be used as internal side for half-cell fabrication. The nature of “roller marks” (a strong example of which can be seen on the calibration disc) is not yet fully elucidated. They possibly are the result of the “conditioning” (i.e. grinding of surface irregularities) performed by the niobium vendors. Note that the roller marks are usually not visible with the naked eye, nor do they appear in profilometric measurements.

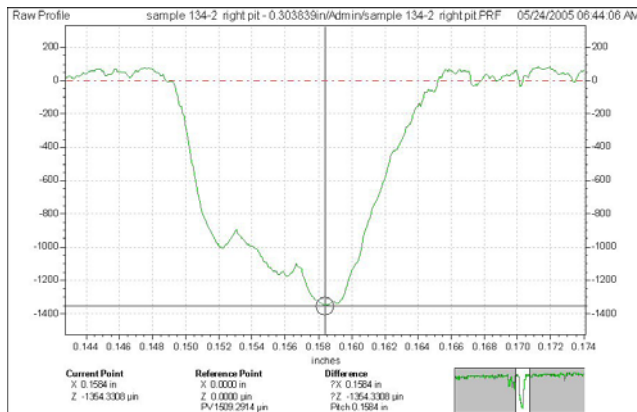


Fig. 7 Typical shape of a pit as detected by a profilometer.

## CONCLUSIONS

Eddy current scanning is now routinely performed at Fermilab. The sensitivity of the device has been considerably improved in terms of alignment of the sensing head and the ability to efficiently analyze the data was optimized by means of additional filtering software. Pits, scratches, and roller marks are the typical defects found, and most of them can be also detected by simple

optical inspection. Part of the defects detected is not eliminated by the subsequent processing of the material.

## ACKNOWLEDGEMENTS

The authors are very thankful to Dan Stout and Norbert Holtkamp from SNS for transfer of the SNS-ECS to Fermilab and to Helen Edwards and Harry Carter for the support of this activity. We would also like to thank Ralph Casperson from BAM for his advice. We are most grateful, however, to Marco Battistoni who conducted most of the ECS measurements presented here as well as Oscar Lira who precision-aligned the scanner and performed the pit measurements. Finally many thanks to Kerry Ewald for designing the probe-height micro-adjustment system, to Luciano Elementi and his team for helping with electrical problems and the air pressure buffer tank, to Charlie Cooper for EDX studies of pits and to Roger Nehring for trouble-shooting the electronics.

## REFERENCES

- [1] W. Singer, D. Proch, A. Brinkmann, “Diagnostic of Defect in High Purity Niobium”, Proceedings of the RF Superconductivity workshop VIII, Abano Terme, Italy, Oct. 1997
- [2] P. Bauer et al., “Eddy-Current Scanner Operating Instructions”, Fermilab, Technical division, internal note TD-04-029, Jun. 2004
- [3] D. J. Hagemaijer, “Fundamentals of eddy current testing”, The American Society For Nondestructive Testing, Feb. 1990
- [4] C. Boffo et al., “FIONDA”, Fermilab, Technical Memo, internal note TM-2313-TD, Jun. 2005
- [5] P. Bauer et al., “Calibration of the SNS Eddy Current Scanner for the Quality Control of the Niobium Blanks for Fermilab's SRF Cavities”, Fermilab, Technical division, internal note TD-05-016, Feb. 2005
- [6] P. Bauer et al., “Eddy Current Scanning Report Fnal – 3<sup>rd</sup> Harmonic Cavity #2”, Fermilab, Technical division, internal note TD-04-039 – rev.1, Mar. 2005
- [7] P. Bauer et al., “Eddy Current Scanning Report FNAL-3<sup>rd</sup> Harmonic Cavities #3-6”, Fermilab, Technical division, internal note TD-05-032, Jun. 2005